Generating Anaglyphs from Light Field Images

Pablo A. Vasquez Guzman
Department of Mechanical Engineering
Stanford University
Stanford, CA
pabloavg@stanford.edu

***Abstract*—Light-field imaging systems have received a lot of attention recently, especially with the release of Lytro cameras for consumer application. Extensive research has been conducted in optimizing and developing applications for light-field images [1,2]. To investigate the potential use of light-field imaging systems as an experimental analysis tool, an automated image processing algorithm was developed to generate anaglyphs images from light-field images acquired from a Lytro Illum camera.**

Keywords—Light-field Images; Anaglyphs; Stereo Image Pairs; Disparity

I. INTRODUCTION

Conventional cameras capture 2D images, which are projections of a 3D scene. Light-field imaging systems capture not only the projection but also the directions of incoming lighting that project onto a sensor. Specifically, Lytro cameras consist of an array of microlenses placed in front of the photosensor used to separate the light rays striking each microlens, and to focus them on different sensors according to their directions as shown in Fig. 1.

Fig. 1. Simplified diagram of a light-field imaging system [3]

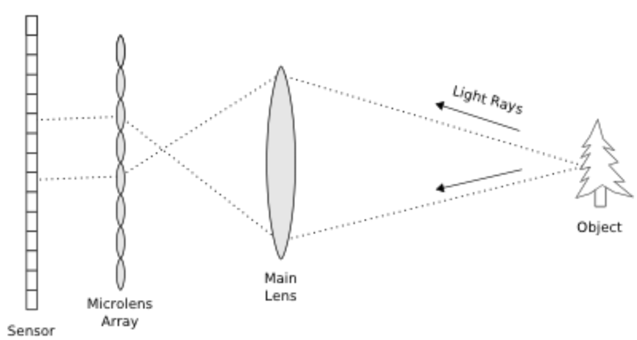

The acquired light-field allows for more flexible image manipulating. Enough information in captured that one can refocus images after acquisition, as well as shift one's viewpoint.

Lytro offers an image processing application, Lytro Desktop, which is a powerful post processing tool for light-field images. One available option is exporting anaglyphs from imported light-field images; however, no information is available on how the anaglyphs are generated. In addition, no prior work is available regarding generating anaglyphs from light-field images.

The standard method for generating anaglyphs requires a pair of images, which have been acquired at slightly different perspective views, called stereo image pairs. Normally, stereo image pairs are acquired using a pair of conventional cameras separated by a distance duplicating the spacing of human eyes. It is possible to create an anaglyph from just one image taken from a conventional camera, but that requires extensive work in a graphics editing program such as Photoshop and it isn't an automated or accurate process.

The specific objective of the work described here was to develop an automated image processing algorithm for generating anaglyphs using the rich information captured in a light-field image acquired from a Lytro Illum camera.

II. METHODS

Two automated image processing algorithms for generating anaglyphs were developed. The first method is based on direct perspective views, while the second method is based on depth-field information.

A. *Method 1*

Lytro uses a hexagonal arrangement of a microlens in front of an image sensor to efficiently capture 4D light field information on a two dimensional plane [2]. The sensor pixels behind the microlens array only records light intensity. Directional information of light is recorded in the location of sensor pixels relative to the microlens array [4]. Stereo image pair can be obtained directly from the raw data to generated an anaglyph. The general process is described below:

1) Calibration and Decoding: Align, color-correct, and rectify raw 2D light-field image to convert the into standard 4D light-field data format as illustrated in Fig. 2.

Fig. 2. Raw 2D light-field image conversion to 4D light-field data format [5]

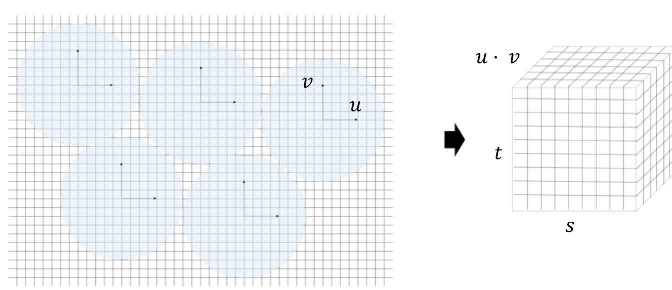

The raw 2D data is converted into $L(s,t,u,v)$ representation, where coordinates (s,t) correspond to each microlens in the array and the coordinates (u,v) correspond to image aperture [4]. The resolution of the raw 2D light-field is about 40-megapixels. For each microlens, the diameter is about 14 pixels. Dividing the raw image resolution by the size of the microlens, the effective resolution of the light-field images is about 0.2-megapixels. Note that Lytro Desktop exports images with 4-megapixel resolution, which indicated that Lytro uses an algorithm to enhance the resolution of its images.

2) Extraction: Extract the left most and right most perspective view images from 4D light-field data. The coordinates *(u,v)* effectively describe viewpoint. Figure 3 shows a simplified diagram of corresponding perspective views extracted from the raw 2D light-field microlens.

Fig. 3. Simplified diagram of a perspective view extraction from raw 2D light-field image [4]

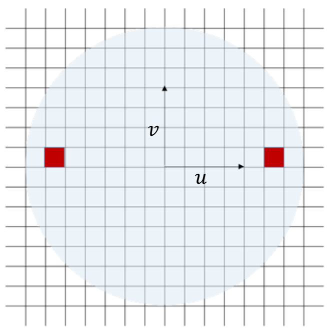

Since the effective resolution of the extracted images are 0.2-megapixels, the images are resized to have about 4-megapixel resolution.

3) Generate Anaglyph: Use left and right extracted perspective views to generate anaglyph.

B. Method 2

Depth-field information can be computed from the light-field image, which can be used to artifically generate stereo image pairs to generated an anaglyph. The general process is described below:

1) Calibration and Decoding: Align, color-correct, and rectify raw 2D light-field image to convert the into standard 4D light-field data format.

2) Depth Map Estimation: Depth can be estimated either from blurred images in a focal stack or from perspective view form a disparity stack. Jeon, et al., describe an effective algorithm to accurately estimate depth map from light-field images based on disparity map [6]. The algorithm developed uses a cost-volume-based methodology.

3) Segmentation: Generating a stereo image pairs requires displacing the focused image according to depth-field information. Displacing each individual pixel requires sub-pixel accuracy to avoid possible artifacts. To minimize artifacts, the depth map is optimally segmented.

Segmentation of the depth map is performed using an optimized multilevel Otsu's method. For *N+1* segments ($N = 1,2,\ldots,20$), the threshold values are computed and a metric is recorded to measure of the effectiveness of the computed thresholds. The depth map is then segment into $N+1$ segments corresponding with metric with the highest effectiveness.

If the number of segments is large ($N > 10$), then the segmentation is refined. The greatest variability in depth values usually occurs in the near- and far-field regions, so first few and last few segments are combined to reduce variability and create a more uniform segmentation.

4) Displacement: The focused image is segmented based on the segmentation of the depth map with the average depth value for each segmented region computed. To obtain stereo pair images requires generating a left and right perspective view. Fig. 4 show how a typical stereo imaging system works

Fig. 4. Geometric schematic explanation of simple stereo system [7]

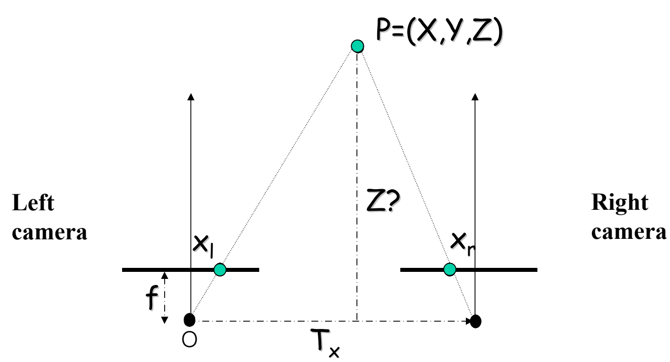

The disparity, d, observed between the left and right view based on some point P is inversly propotional to the depth.

$$d = f \cdot T_x / Z \tag{1}$$

where f is the focal length, T_x is the distance between the views, and Z is the depth. Based on the computed depth values, the image segments are displaced accordinly to generate a left and right perspective view.

5) Hole Removal: Due to the uneven displacement of segmented regions of the image and occlusion of objects in the image, holes are typically generated in the process of generating the stereo pair images. Proper removal of these holes is necessary to minimize artifacts. The hole removal process is described below:

a) Detection: Convert the stereo image pairs to gray scale and apply Otsu's method to binerize image into indicating region without any information.

b) Filling: Dilate binary hole image to create a mask, which include surrounding pixel values around all hole regions. Use surrounding average pixel intensity values to fill in hole region values.

6) Anaglyph Generation: Use left and right generated perspective views to generate anaglyph.

III. Results

A. Method 1

The light-field images acquired from a Lytro Illum camera were calibrated and decoded using Light Field Toolbox for Matlab developed by Donald G. Dansereau. Fig. 5 shows the intermediate results in applying the image processing algorithm for an example light-field image.

Fig. 5. Intermetiate results of first image processing algorithm applied to an example light-field image

1) Calibration and Decoding…

2) Extraction:

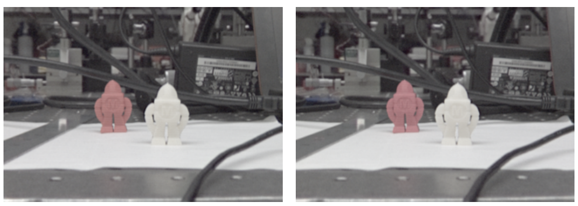

3) Generate Anaglyphs

Fig. 6 shows the final results of generating anaglyphs for some of the accessible light-field images. Note that the color-correction applied didn't properly balance the colors in the images. The applied color-correction was an shades-of-gray technique, but a more robust color-correction technique is needed to generate results similar to those generated by Lytro Desktop.

Fig. 6. Results of first automated image processing algorithm method

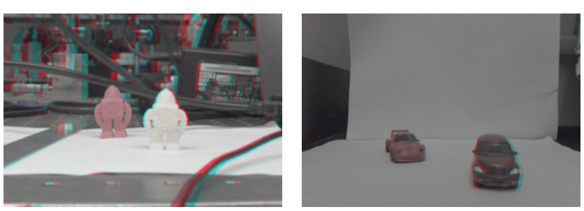

B. Method 2

Unfortunately, an accurate depth map was unable to be computed from the light-field images using the described methodology. More rudimentary attempts of computing depth maps were attempted, but the results were unsatisfactory. The anaglyphs results shown below were generated using the depth map and focused image exported from Lytro Desktop. Fig. 7 show intermediate result of the image processing algorithm for one light-field image.

Fig. 7. Intermetiate results of second image processing algorithm applied to an example light-field image

1) Calibration and Decoding…

2) Depth Map Estimation…

3) Segmentation and Refinement:

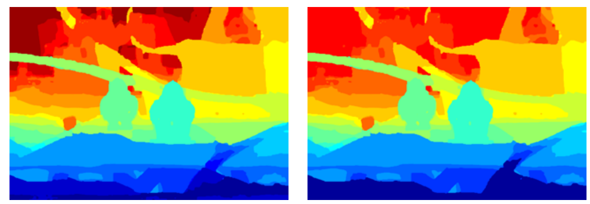

4) Displacement:

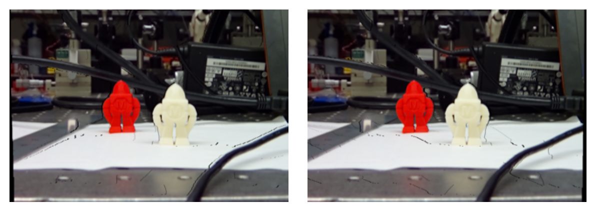

5) Fill Holes:

a) Detection:

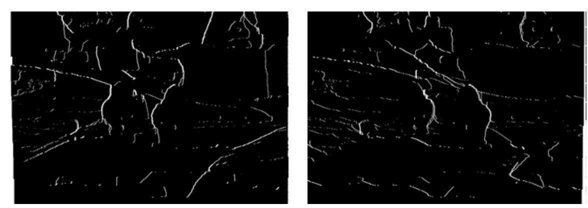

b) Filling:

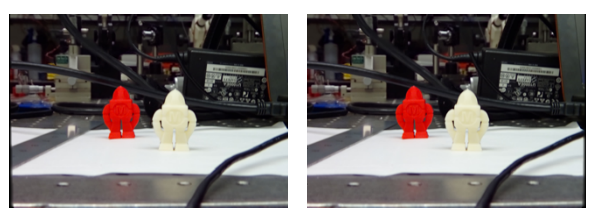

6) Generate Anaglyph:

Fig. 8 shows the final results of generating anaglyphs for all the accesibale light-field images. Using 3D red/cyan glasses, the results can be seen clearly.

Fig. 8. Results of second automated image processing algorithm method

IV. Discussion

The two automated image processing algorithms developed for generating anaglyphs produce desirable results. The disparity in the stereo image pairs obtain from the first method were expected to be too small to a generated an anaglyph; however, the observed disparity is sufficient enough to observe a noticeable difference and produce desirable results. While the first method provides the simplest method for generating anaglyphs note that there is degradation in image quality applying this method. The microlens has non-uniform effects which greatly degrade the extracted light-field images from the border sensor pixels relative to the microlens.

While the second automated image processing algorithm method produced desirable results, it is very dependent on obtain an accurate depth map estimation. An inaccurate or noisy depth map estimation would lead to lots of artifacts and discrepancies in the generated anaglyph. Generating both stereo image pairs rather than one relative to the other greatly helped minimize artifacts that would be otherwise amplified by the hole filling process.

A. Comparison

Lytro Desktop offers the option to export anaglyphs from imported light-field images. Fig. 9 shows a comparison between the anaglyphs generated from the second automated image processing algorithm method vs. those obtain from Lytro Desktop.

Fig. 9. Comparison of results (left) with Lytro Desktop (right)

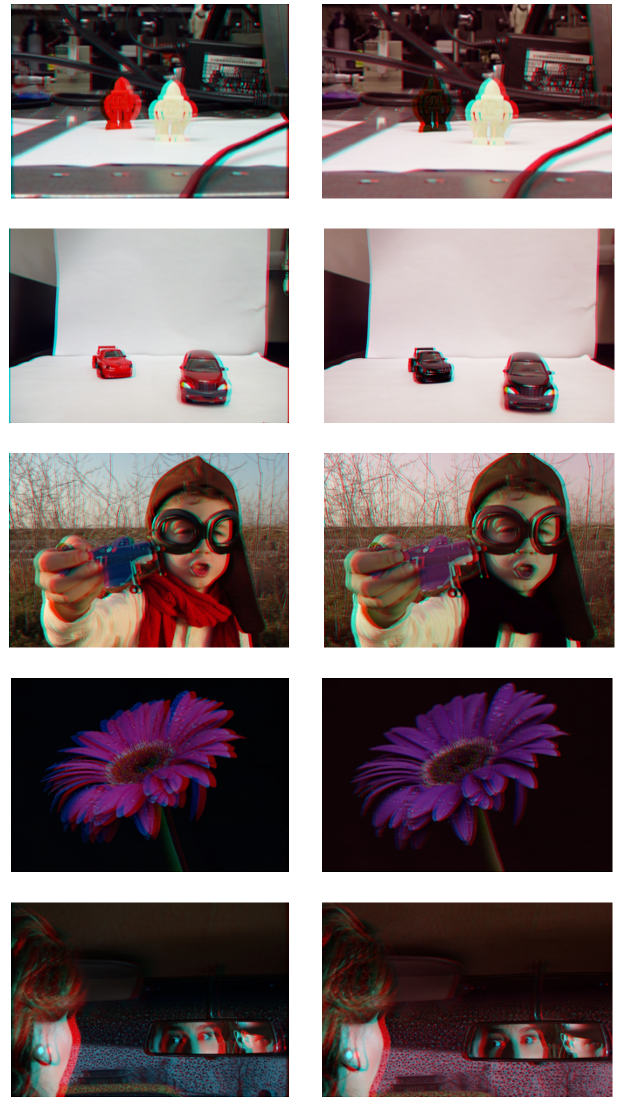

Beside the color filtering difference in generating the anaglyphs, qualitatively the anaglyphs obtain from the Lytro Desktop are very similar to the results obtain from the second automatic image processing algorithm method, which indicate that Lytro might use a similar algorithm to generate their anaglyphs.

B. Limitations

Another challenge besides obtaining an accurate depth map estimation are the holes generated by displacing occlusions. The hole filling process produced desirable results with very minimal artifacts. In order to investigate the limitation of the image processing algorithm, the disparity between the stereo image pairs were increased by a factor of 2, 4, 6, 8, 10, and 12 the results of which for one light-field image are shown in Fig. 10.

Fig. 10. Results from increasing disparity by factor of 2, 4, 6, 8 10 and 12

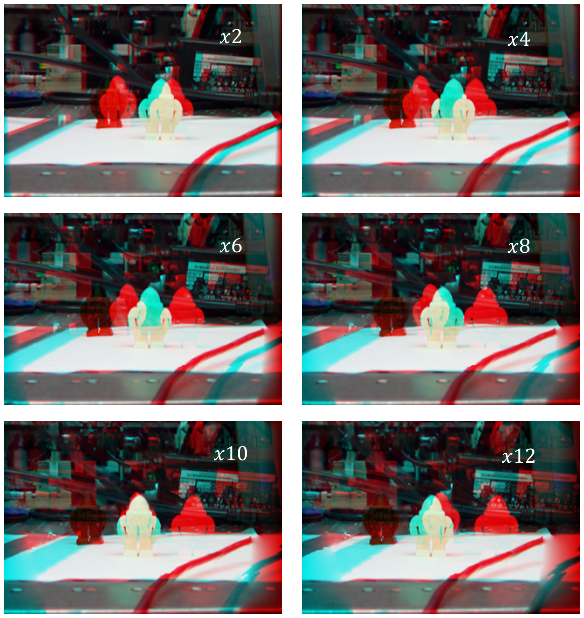

Artifacts become pronounced once the disparity is increased by a factor of 8, especially for objects in the image that span various depth fields. The holes become large due to the increased displacement that they are no longer properly filled. A different hole filling technique can be implements to reduce artifacts for large displacements, but unnecessary in the interest of generating anaglyphs.

V. Conclusion

The automated image processing algorithms developed are robust under different imaging conditions. The results obtain by applying the second automated image processing algorithm method agrees well with those obtained directly from Lytro Desktop. However, the results depend greatly on computing an accurate depth map estimation. Future work requires the development of an accurate depth map estimator.

Even though acquired light-field images allows for more flexible image manipulation, the spatial resolution is significantly reduced at the cost of gaining angular resolution. The use for light-field imagining systems as an experimental analysis tool is currently limited due to the degradation of spatial resolution and sensitivity of depth map estimation as discovered from this project.

Acknowledgment

The author would like to thank Professor Gordon Wetzstein for his guidence on this project and the teaching staff of EE368: Digital Image Processing for their contribution in the course.

References

[1] T. Georgiev, Z. Yu, A. Lumsdaine, and S. Goma, "Lytro camera technology: theory, algorithms, performance analysis," In Proceedings of SPIE, Multimedia Content and Mobile Devices, 2013.

[2] D. Cho, M. Lee, S. Kim, and Y. Tai, "Modeling the Calibration Pipeline of the Lytro Camera for High Quality Light-Field Image Reconstruction", International Conference on Computer Vision, Sydney, Australia, 2013.

[3] M. Hansen and E. Holk, "Depth map estimation for plenoptic images," 2011.

[4] H. Zhang, "3D Surface Reconstruction Based On Plenoptic Image," M.S. thesis, ELCE Dept., Auburn Univ., Auburn, Alabama, 2015.

[5] D. Johnston, "Learning Depth in Light Field Images," unpublished.

[6] H. Jeon et al., "Accurate Depth Map Estimation from a Lenslet Light Field Camera,"In Proceedings of International Conference on Computer Vision and Pattern Recognition, 2015.

[7] G. Wetzstein. EE 368. Class Lecture, Topic: "Panoramic Imaging – Part 2: Stereo Panoramas." Stanford University, Stanford, California, Nov., 2015.